The Journal of Immunology

SARM Is Required for Neuronal Injury and Cytokine Production in Response to Central Nervous System Viral Infection

Ying-Ju Hou, Rebecca Banerjee, Bobby Thomas, Carl Nathan, Adolfo García-Sastre, Aihao Ding and Melissa B. Uccellini

J Immunol 2013; 191:875-883; Prepublished online 7 June 2013;
doi: 10.4049/jimmunol.1300374
http://www.jimmunol.org/content/191/2/875

The Journal of Immunology is published twice each month by
The American Association of Immunologists, Inc.,
9650 Rockville Pike, Bethesda, MD 20814-3994.

Print ISSN: 0022-1767 Online ISSN: 1550-6606.

SARM Is Required for Neuronal Injury and Cytokine Production in Response to Central Nervous System Viral Infection

Ying-Ju Hou,* Rebecca Banerjee,† Bobby Thomas,‡,§ Carl Nathan,* Adolfo García-Sastre,¶,‖,# Aihao Ding,* and Melissa B. Uccellini¶

Four of the five members of the Toll/IL-1R domain–containing adaptor family are required for signaling downstream of TLRs, promoting innate immune responses against different pathogens. However, the role of the fifth member of this family, sterile α and Toll/IL-1R domain–containing 1 (SARM), is unclear. SARM is expressed primarily in the CNS where it is required for axonal death. Studies in *Caenorhabditis elegans* have also shown a role for SARM in innate immunity. To clarify the role of mammalian SARM in innate immunity, we infected *SARM*$^{-/-}$ mice with a number of bacterial and viral pathogens. *SARM*$^{-/-}$ mice show normal responses to *Listeria monocytogenes*, *Mycobacterium tuberculosis*, and influenza virus, but show dramatic protection from death after CNS infection with vesicular stomatitis virus. Protection correlates with reduced CNS injury and cytokine production by nonhematopoietic cells, suggesting that SARM is a positive regulator of cytokine production. Neurons and microglia are the predominant source of cytokines in vivo, supporting a role for SARM as a link between neuronal injury and innate immunity. *The Journal of Immunology*, 2013, 191: 875–883.

The innate immune system relies on TLRs as well as a number of other pattern recognition receptors to detect pathogen-associated molecular patterns. The TLRs signal through the Toll/IL-1R (TIR) domain–containing adaptor protein family, which includes MyD88, TRIF, MAL, and TRAM. Each of these family members plays positive roles in innate immunity by inducing the expression of IFN-β or activation of NF-κB, and deficiency leads to increased susceptibility to infection. Sterile α and TIR domain–containing 1 (SARM) is the fifth member of the family to be identified, and it is composed of seven N-terminal HEAT/Armadillo motifs, two central sterile α motifs, and a C-terminal TIR domain (1), and is highly conserved between fly, worm, and mammals (2).

In *Caenorhabditis elegans*, TOL-1 is the sole TLR homolog and the SARM homolog TIR-1 is the sole cytoplasmic TIR-domain containing protein (3). TIR-1 knockdown worms display increased susceptibility to fungal infection and decreased antimicrobial peptide synthesis, supporting a positive role for SARM in innate immunity in worms. However, this susceptibility was not dependent on TOL-1 (4), suggesting that SARM may not only function as a TLR adaptor. TIR-1 is also expressed in *C. elegans* olfactory neurons where it regulates olfactory patterning. Genetic evidence suggests TIR-1 mediated patterning through a UNC-43(CaMKII)→TIR-1(SARM)→NSY(ASKI MAPKKK)→PMK-1(p38/JNK) pathway (5). Whether this pathway is also involved in the innate immune phenotype is unknown.

In contrast with results in *C. elegans*, human SARM has been suggested to function as a negative regulator of TRIF signaling in myeloid cells. Overexpression of SARM in 293T cells was shown to inhibit TRIF-dependent TLR signaling. In addition, LPS treatment of human PBMCs led to increased expression of SARM (6). However, when *SARM*$^{-/-}$ mouse macrophage TLR responses were tested, they failed to show defects in cytokine production. This may be explained by the predominant expression of SARM at the RNA level in human and mouse brain, and relatively low expression in myeloid cells (7). Consistent with CNS expression, SARM has been reported to mediate stress-induced cell death, as neurons from *SARM*$^{-/-}$ mice are protected from glucose deprivation–induced death (7). In addition, *SARM*$^{-/-}$ mice infected with West Nile virus showed decreased TNF-α production and increased susceptibility to infection supportive of a positive role for SARM in innate immunity in mammals (8). Thus, SARM expression can be either detrimental or protective depending on the context.

Recent evidence has identified SARM as a mediator of an active axonal destruction program termed Wallerian degeneration (9). After injury to axons, neurons undergo degeneration distal to the injury site and a coordinated sequence of events leads to clearance of necrotic debris, degeneration, and subsequent axonal regeneration (10). *SARM*$^{-/-}$ axons were protected from Wallerian degeneration, and the synaptic termini at the neuromuscular junctions were preserved after transection (9). After trauma, cytokines and chemokines are

*Department of Microbiology and Immunology, Weill Medical College of Cornell University, New York, NY 10021; †Department of Neurology and Neuroscience, Weill Medical College of Cornell University, New York, NY 10021; ‡Department of Pharmacology and Toxicology, Georgia Health Sciences University Medical College of Georgia, Augusta, GA 30912; §Department of Neurology, Georgia Health Sciences University Medical College of Georgia, Augusta, GA 30912; ¶Department of Microbiology, Icahn School of Medicine at Mount Sinai, New York, NY 10029; ‖Division of Infectious Diseases, Department of Medicine, Icahn School of Medicine at Mount Sinai, New York, NY 10029; and #Global Health and Emergent Pathogens Institute, Icahn School of Medicine at Mount Sinai, New York, NY 10029

Received for publication February 8, 2013. Accepted for publication May 17, 2013.

This work was supported by National Institutes of Health Grant NS060885 (to B.T.) and National Institute of Allergy and Infectious Diseases Grant U19AI083025 (to A.G.S.).

The microarray data presented in this article have been submitted to National Center for Biotechnology Information Gene Expression Omnibus (http://www.ncbi.nlm.nih.gov/geo/) under accession number GSE44331.

Address correspondence and reprint requests to Dr. Melissa B. Uccellini, Department of Microbiology, Icahn School of Medicine at Mount Sinai, 1 Gustave Levy Place, Box 1124, New York, NY 10029. E-mail address: melissa.uccellini@mssm.edu

The online version of this article contains supplemental material.

Abbreviations used in this article: MOI, multiplicity of infection; qRT-PCR, quantitative RT-PCR; SARM, sterile α and Toll/IL-1R domain–containing 1; TIR, Toll/IL-1R; WT, wild-type.

produced locally by cells including microglia and oligodendrocytes, leading to the infiltration of glial cells and macrophages that remove axonal and myelin debris. This process is thought to aid in cytoskeletal rearrangements leading to growth cones and regeneration (11). The Wld^s mouse, which displays a delayed Wallerian degeneration phenotype similar to *SARM*$^{-/-}$ mice, is also deficient in cytokine production, suggesting that the processes are intricately linked (12). In addition to promoting repair of damaged brain tissue, glial activation and cytokine production in the CNS may injure bystander cells (13, 14). In other organs, this collateral damage is typically reversible, because of the regenerative capacity of the tissue, but repopulation of cells is limited in the CNS (15). Therefore, establishing a balance between the protective and destructive effects of the neuroinflammatory response in the brain is critical (16, 17), and SARM may play a role in this balance.

In this study, we challenged *SARM*$^{-/-}$ mice with various pathogens to better understand the role of SARM in innate immune responses and disease. Consistent with a role of SARM in neurodegeneration, we found that vesicular stomatitis virus (VSV)–infected *SARM*$^{-/-}$ mice were protected from neurodegeneration and neuropathology. In addition, *SARM*$^{-/-}$ mice showed dramatically reduced cytokine and chemokine production in the brain after VSV challenge, supporting a positive role for SARM in cytokine production similar to its *C. elegans* homolog. In vivo and in vitro data suggest that cytokine production is mediated by CNS resident cells and relies on the cooperation between neurons and microglia. Collectively, these data support the role of SARM in neurodegeneration and suggest that SARM is a link between innate immune responses and neurodegeneration.

Materials and Methods

Mice

SARM$^{-/-}$ mice on the C57BL/6J background were generated previously (7) and compared with wild-type (WT) C57BL/6J mice purchased from The Jackson Laboratory. Animal studies were approved by the Institutional Animal Care and Use Committee of Weill Medical College of Cornell University and/or Icahn School of Medicine at Mount Sinai.

Bacterial infections

Eight-week-old mice were i.v. infected with 5×10^3 *L. monocytogenes*. Livers were homogenized in a 0.3% collagenase solution (Collagenase Type IV; Worthington) and plated on Brain Heart Infusion agar plates to determine bacterial burden. Using an Inhalation Exposure System (Glas-Col), 6 ml *Mycobacterium tuberculosis* at OD = 0.15_{580} ($\sim 7.5 \times 10^6$ bacteria) was nebulized for 40 min, which correlates with ~100 bacteria implanting. Lungs were homogenized and plated on 7H11 agar to determine bacterial burden.

Viral infections

Six- to 8-wk-old animals were anesthetized with ketamine/xylazine and infected intranasally with 10^7 PFU VSV-Indiana or 100 PFU influenza A/PR/8/34 virus in 20 μl PBS. For intracranial infections, 5-wk-old mice were injected with 50 PFU in 30 μl in the parietal lobe, slightly in front of the bregma. Mice were monitored daily for weight and sacrificed when exhibiting severe paralysis or >25% weight loss. Organs were homogenized (MP Biomedical) in 0.2% BSA/PBS. VSV titers were determined on BHK cells with Avicel overlay (18); influenza titers were determined on MDCK cells with oxoid agar overlay and crystal violet staining.

Pathology

Mice were perfused with 4% PFA/PBS. Brains were fixed overnight (ON) in 4% PFA/PBS, paraffin embedded, and sectioned at the Histology Shared resource facility at Icahn Medical School at Mount Sinai. Serial sections were stained for H&E, VSV, or TUNEL. For VSV immunohistochemistry, sections were deparaffinized followed by Ag retrieval in Citra plus solution (Biogenex). Sections were blocked with 4% goat serum and incubated with rabbit polyclonal anti–VSV-G (Abcam) followed by anti-rabbit IgG(H+L)-bio, ABC kit, Nova red staining (Vector Laboratories), and hematoxylin counterstain. TUNEL staining was performed using the DeadEnd Colorometric TUNEL System (Promega). Pathology was scored blindly by the Comparative Pathology Diagnostic Laboratory of the Icahn Medical School at Mount Sinai as follows: 1 = mild, few inflammatory cells, focal or multifocal, <5 cells thick; 2 = moderate, multifocally affected, inflammation is 5–10 cells thick; and 3 = severe, multifocally affected, >10 cells thick, spreading into parenchyma. Points were given for necrosis or meningitis detected, and a total score was calculated for sagittal brain sections from each hemisphere. For Fluoro-Jade staining, brains were fixed for 2 h in 4% PFA, ON in 4% PFA/20% sucrose, frozen in OCT, and sectioned. Slides were stained in Fluoro-Jade C (Chemicon) according to the manufacturer's protocol. For MCP-1 immunohistochemistry, mice were perfused with PBS and 4% PFA/PBS, and brains were fixed ON in 4% PFA/30% sucrose/PBS. Paraffin sections were blocked with 10% goat serum and stained with rabbit polyclonal anti–MCP-1 (Millipore), anti-rabbit biotin (Jackson Immunoresearch), streptavidin-HRP, and 3,3′-Diaminobenzidine substrate (Sigma). For MCP-1 immunofluorescence, mice were perfused with PBS and formalin-free Zinc fixative (BD Biosciences), and 5-mm sections were incubated ON in fixative. Samples were paraffin embedded and sectioned at the Electron Microscopy & Histology core facility at Weill Cornell Medical College. Sections were deparaffinized and stained with rabbit polyclonal anti–MCP-1 (Millipore), mouse anti-CD11b (Serotec), mouse anti-GFAP (Covance), and anti-mouse Alexa488 and anti-rabbit IgG Alexa 594 (Molecular Probes).

Quantitative RT-PCR and ELISA

Total RNA was isolated from perfused brain and lung with the RNeasy kit (Qiagen), and reverse transcribed with Oligo dT using MuLV reverse transcriptase (Perkin Elmer). cDNA was used for PCR with gene-specific primer and probes (BioSearch) using the ABI PRISM 7900HT sequence detection system (Perkin Elmer). MIP-1α, MCP-1, and RANTES ELISAs were from R&D Systems.

Infiltration and flow cytometry analysis

Mice were perfused with PBS, and brains were mashed through a 70-μM filter in 0.06% BSA/300 μM EDTA/Hanks. Leukocytes were isolated on a 30%/70% Percoll gradient (GE Healthcare) after centrifugation at 2500 rpm for 30 min. Cells were washed and incubated with UV LIVE/DEAD stain (Invitrogen); anti–CD11b-allophycocyanin-Cy7, anti–CD19-FITC, anti–CD4-allophycocyanin-Cy7, and anti–CD8-PE-Cy7 (BD Pharmingen); and anti–CD45-allophycocyanin and anti–NK1.1-allophycocyanin (eBioscience). Cell number was quantified by flow cytometry using AccuCount Particles (Spherotech), and plots were gated on live cells. Flow cytometry was performed on a BD LSRII.

Bone marrow chimeras

Six-week-old B6.SJL-*Ptprc*^{a} *Pepc*^{b}/BoyJ (CD45.1) and *SARM*$^{-/-}$ (CD45.2) mice were irradiated with two doses of 600 rad. Bone marrow cells from WT (CD45.2) or *SARM*$^{-/-}$ donor mice were prepared, and 10^7 donor cells were i.v. injected into recipient mice 4 h after irradiation. Reconstitution (95%) was confirmed by flow cytometry 6 wk later, and mice were infected 2 wk later.

Neuronal cell culture

Primary hippocampal neurons were generated from embryonic day 15–17 embryos using previously described methods (19) and plated at 1.5×10^5 cells in 24-well PureCoat plates (BD Biosciences) in Neurobasal media supplemented with B27 and GlutaMAX (Invitrogen). Primary microglia were isolated from astrocyte monolayers from postnatal day 1 mice (19) in the presence of 5 ng/ml M-CSF (R&D Systems) and removed by shaking at 125 rpm for 4 h. Astrocytes were isolated from the same cultures by trypsinization after microglia were removed. Bone marrow–derived macrophages were cultured for 6 d in DMEM supplemented with 20% L929 cell media. For mixed cultures, neurons were allowed to differentiate for 3 d in vitro, before microglia, astrocytes, or bone marrow–derived macrophages were directly added to neurons at a 10:1 ratio of neurons to other cells. Eighteen hours after mixing, cells were infected with VSV at multiplicity of infection (MOI) 1 for 30 min, and supernatants were harvested at 8 h postinfection.

Microarray

Mice were infected intranasally with 10^7 PFU VSV; at day 5 postinfection, mice were perfused with PBS, brains were harvested, and RNA was prepared by TRIzol extraction. Triplicate samples of three pooled mice were analyzed at the Biopolymers Facility at Harvard Medical School on the Mouse 430 2.0 chip (Affymetrix). Genes significantly different between WT and *SARM*$^{-/-}$ VSV-infected mice were determined using Genepattern,

and results were deposited in National Center for Biotechnology Information Gene Expression Omnibus (accession no. GSE44331, http://www.ncbi.nlm.nih.gov/geo/).

Results

SARM$^{-/-}$ *mice show normal responses to* Listeria, M. tuberculosis, *and influenza virus but are protected from VSV*

To determine whether SARM has a role in innate immunity similar to the other TIR-domain–containing adapters, we infected *SARM*$^{-/-}$ mice with various bacterial and viral pathogens. Bacterial burdens of *SARM*$^{-/-}$ mice in response to *M. tuberculosis* were similar to WT animals (Fig. 1A), as were responses to *Listeria* (Fig. 1B). *SARM*$^{-/-}$ mice also showed similar susceptibility to influenza virus and similar viral titers in the lung (Fig. 1C).

To determine whether SARM plays a unique role in the innate immune response in the brain, given its expression in the CNS (7), we next studied responses to VSV, a member of the family *Rhabdoviridae*, commonly used as a model to study neurotropic viral infection. Surprisingly, *SARM*$^{-/-}$ mice showed dramatic protection from intranasal VSV infection at a range of infectious doses (Fig. 1D, Supplemental Fig. 1). This protection was not due to differences in viral titers in the brain or lung (Fig. 1D). To exclude possible differences in neuroinvasion similar to TLR3 deficiency (20), and to directly address whether the unique phenotype with VSV infection was related to CNS infection, we inoculated mice intracranially with VSV. Using this method, we observed the same enhanced survival phenotype in *SARM*$^{-/-}$ mice, indicating that CNS infection with VSV results in increased survival in *SARM*$^{-/-}$ mice and suggesting neuroinvasion did not account for the observed difference in susceptibility. This phenotype was again independent of viral load in the brain (Fig. 1E), suggesting differences in the immune response contributed to the enhanced survival of *SARM*$^{-/-}$ mice. Both intranasal and intracranial VSV infection led to tail and hind limb paralysis and labored breathing that occurred with rapid onset between days 4 and 9 postinfection. Symptoms were similar in both WT and *SARM*$^{-/-}$ animals that succumbed to infection; however, the occurrence of symptoms and lethality was less common in *SARM*$^{-/-}$ mice. Animals that survived infection either showed no symptoms or signs of mild tail or hind-limb paralysis that did not persist beyond 14 d postinfection.

SARM$^{-/-}$ *mice show reduced pathology in the brain*

To compare the extent of neuronal damage, we next examined histological sections from WT and *SARM*$^{-/-}$ mice. Because WT mice succumb to disease with variable kinetics, brains were harvested between days 6 and 10 postinfection when animals showed signs of paralysis. *SARM*$^{-/-}$ animals with similar symptoms were harvested when available. WT animals showed multifocal necrosis and meningitis (11/11 and 10/11, respectively; Fig. 2D), but *SARM*$^{-/-}$ mice showed reduced incidence of pathology (4/11 necrosis and 6/11 meningitis), and pathology was also less severe when present (Fig. 2B, 2D). In serial sections from WT mice, we observed loss of cell architecture, eosinophilia of the cytoplasm, and appearance of pyknotic and karyorrhectic nuclei under H&E staining (Fig. 2A, top) as well as TUNEL staining indicative of necrosis in sections that stained positive for VSV Ag. However, although we did observe some necrosis in *SARM*$^{-/-}$ brain (Fig. 2D), we also observed several areas that stained positive for VSV Ag but showed no signs of necrosis under H&E or TUNEL staining (Fig. 2A, middle). In addition, WT mice had a higher

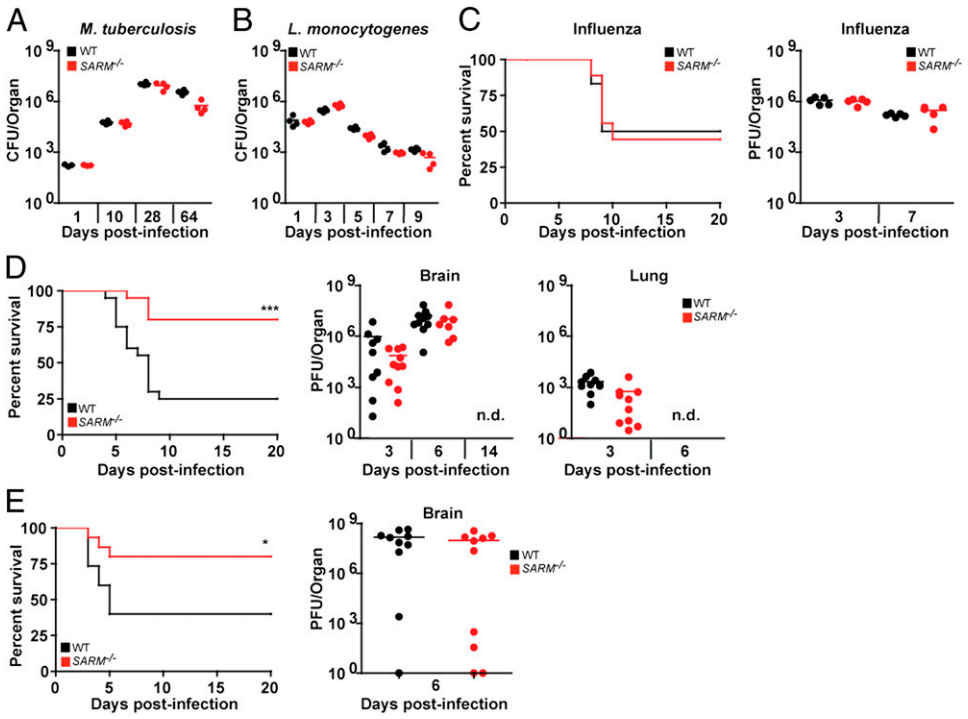

FIGURE 1. *SARM*$^{-/-}$ mice are protected from VSV infection. (**A**) WT and *SARM*$^{-/-}$ mice infected with nebulized *M. tuberculosis* have similar bacterial load in the lungs ($n = 4$ per time point). (**B**) Similar bacterial burden in livers of WT and *SARM*$^{-/-}$ mice infected i.v. with 5×10^3 CFU *L. monocytogenes* ($n = 4$ per time point). (**C**) WT and *SARM*$^{-/-}$ mice have similar survival rates ($n = 10$) and viral titers in lungs ($n = 5$) after intranasal infection with 100 PFU A/PR/8/34 influenza virus. (**D**) WT and *SARM*$^{-/-}$ mice were intranasally infected with 10^7 PFU VSV and monitored daily for mortality ($n = 20$). Brains and lungs were harvested to determine viral burden by plaque assay ($n = 9$–10). PFU data shown were pooled from two independent experiments. (**E**) *SARM*$^{-/-}$ mice intracranially infected with 50 PFU VSV have decreased mortality as compared with WT animals, but viral burdens in the brains of *SARM*$^{-/-}$ mice were comparable with that of WT ($n = 10$). Bars represent mean bacterial or viral titers. For (D) and (E), $*p < 0.02$ and $***p < 0.0002$ compared with WT mice, Student t test. n.d., Not detected.

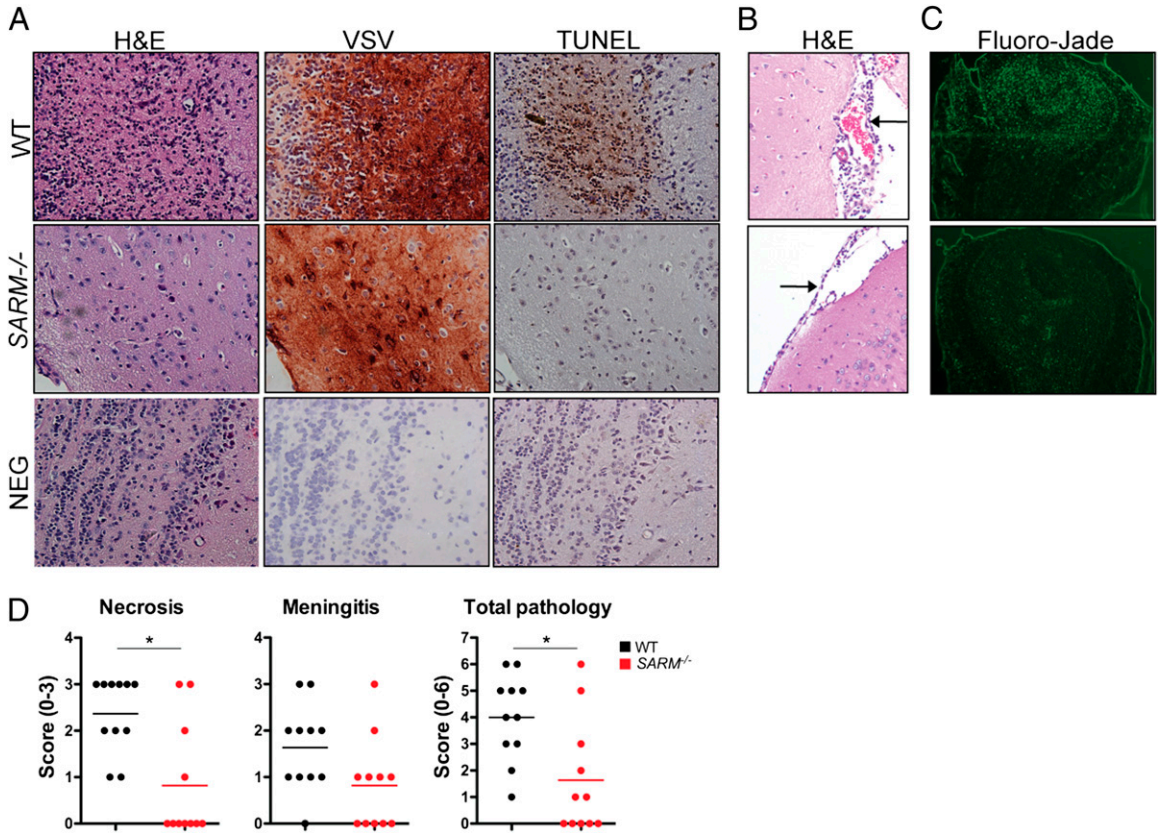

FIGURE 2. *SARM*$^{-/-}$ mice show reduced pathology in the brain. (**A**) Brain sections from WT (necrosis score 3) and *SARM*$^{-/-}$ (necrosis score 0) mice infected intranasally with VSV were stained for H&E, VSV, or apoptosis by TUNEL staining at day 5 postinfection showing the presence of VSV but absence of necrosis and TUNEL staining in *SARM*$^{-/-}$ brain. Original magnification ×40. (**B**) H&E staining showing severe meningitis of WT (score 3) and mild meningitis of *SARM*$^{-/-}$ (score 1) brain. Original magnification ×40. Arrows indicate inflammation of the meninges. (**C**) Olfactory bulb sections were stained for Fluoro-Jade ($n = 4$). Original magnification ×10. (**D**) Pathology for necrosis, meningitis, and total pathology ($n = 11$) was scored as described in *Materials and Methods*. *$p < 0.02$.

incidence of more severe meningitis as indicated by expansion of the leptomeninges and accumulation of high numbers of inflammatory cells (Fig. 2B, top) as compared with milder meningitis observed in *SARM*$^{-/-}$ mice (Fig. 2B, bottom). We also observed less neurodegeneration in *SARM*$^{-/-}$ animals in the olfactory bulb, which is the site of initial VSV replication and spread to the brain (21) (Fig. 2C), suggesting that neural tissue is protected from degeneration in *SARM*$^{-/-}$ mice during VSV infection, as previously reported during axonal injury (9).

SARM$^{-/-}$ *mice have reduced cytokines and infiltration in the brain*

To determine whether there was a difference in the inflammatory response between WT and *SARM*$^{-/-}$ animals post-VSV infection, we isolated RNA from brain and lung homogenates at day 6 postinfection and tested a number of chemokines and cytokines by quantitative RT-PCR (qRT-PCR). Many inflammatory mediators are produced post intranasal infection with VSV including chemokines such as MCP-1 and RANTES, as well as cytokines such as type I IFNs and TNF-α (22, 23). *SARM*$^{-/-}$ mice had severely blunted responses to all cytokines and chemokines examined in the brain (Fig. 3A), but had similar levels to WT in the lung (Supplemental Fig. 2). In addition, levels of MIP-1α, MCP-1, and RANTES protein were also significantly reduced in *SARM*$^{-/-}$ brains compared with WT. In contrast with the RNA data, we were unable to detect TNF-α protein in brain homogenates (Fig. 3B). Microarray analysis on brain samples also corroborated these results. WT mice showed significantly higher upregulation of a number of chemokines and IFN-inducible genes as compared with *SARM*$^{-/-}$ animals (Fig. 3C, Table I), confirming that SARM expression is important for the initiation of the innate immune response in the brain post VSV infection. Given the lack of type I IFN in the brains of *SARM*$^{-/-}$ mice, it was surprising that we did not observe differences in viral replication (Fig. 1D). Analysis of the microarray data set showed that *SARM*$^{-/-}$ mice did produce levels of IFN-inducible genes above PBS controls, although they failed to upregulate these genes to the same extent as WT mice (Fig. 3C). This may indicate that low levels of type I IFN were present and sufficient to control viral replication. XIAP-associated factor, Xaf1, was highly upregulated in *SARM*$^{-/-}$ animals compared with WT; however, Western blot failed to show any change in Xaf1 levels (data not shown).

Given the differences in chemokines, we next examined recruitment of inflammatory cells into the brain postinfection. Consistent with published results and our histological examination (Fig. 2A), we saw more infiltrating leukocytes in the brains of VSV-infected mice at day 7 postinfection, but there was a decrease in the total number of cells in the brains of infected *SARM*$^{-/-}$ mice (1×10^6) compared with WT mice (1.5×10^6; Fig. 3D). Using flow cytometry, we found significantly fewer macrophages and monocytes in *SARM*$^{-/-}$ brains than in WT brains (Fig. 3E). In addition, *SARM*$^{-/-}$ mice showed a trend of decreased neutrophils, CD4$^+$ T cells, and CD8$^+$ T cells (Fig. 3E, 3F), although the differences were not statistically significant at this time point.

Although VSV-associated neuropathogenesis is reported to be T cell independent, CD4$^+$ and CD8$^+$ T cells are required for viral

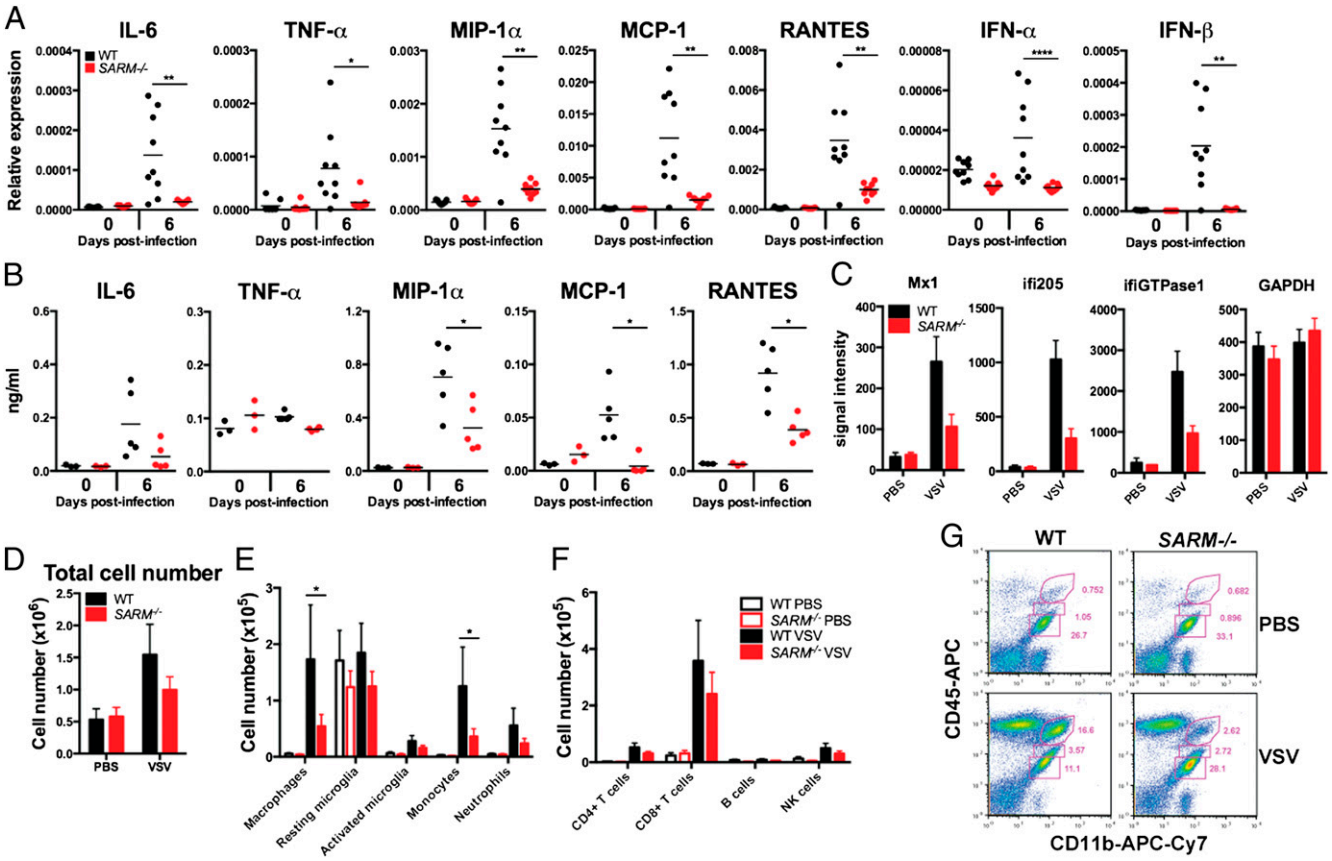

FIGURE 3. *SARM*$^{-/-}$ mice show reduced cytokines and infiltration in the brain. (**A**) qRT-PCR results from intranasally VSV-infected mouse brains expressed relative to GAPD ($n = 9$, representative data from two independent experiments). (**B**) Whole-brain homogenates were assayed for the production of chemokines by ELISA ($n = 5$, representative data from 2 independent experiments). (**C**) Mas5.0 signal intensity for selected genes from microarray. (**D**) Leukocytes were isolated by Percoll gradient centrifugation at day 7 postinfection and quantified by flow cytometry. (**E**) Cells were stained with CD11b, CD45, and Ly6C, and populations were analyzed by flow cytometry (macrophages CD11b^{hi}CD45^{hi}, resting microglia CD11b^{lo}CD45^{lo}, activated microglia CD11b^{int}CD45^{int}, monocytes CD11b^{+}Ly6C^{+}, and neutrophils CD11b^{+}Ly6Cint). (**F**) Cells were stained with CD4, CD8, CD19, and NK1.1 to analyze CD4^{+} and CD8^{+} T cells, CD19^{+} B cells, and NK1.1^{+} NK cells. (**G**) Representative FACS plot showing percentages of macrophages, resting microglia, and activated microglia. For (A) and (B), bars represent mean. For (D)–(F), data are from six to seven mice per group, and error bars show SEM. $*p < 0.05$, $**p < 0.005$, $****p < 0.00005$ compared with WT mice, Student t test.

clearance and host recovery (21). In addition to expression in the CNS, low levels of SARM were also detected in CD3^{+} splenocytes (7). *SARM*$^{-/-}$ mice also showed no differences in CD4^{+} or CD8^{+} T cell numbers in the thymus, spleen, or lymph nodes, and *SARM*$^{-/-}$ splenocytes proliferated normally in response to anti-CD3/anti-CD28 (Supplemental Fig. 3), indicating that SARM is dispensable for T cell development. Decreased numbers of activated microglia have been observed in *SARM*$^{-/-}$ mice during West Nile virus infection (8). We did observe a trend of less activated microglia (CD11b^{int}CD45^{int}) in *SARM*$^{-/-}$ mice (Fig. 3E, 3G); however, the differences were not statistically significant at this time point.

SARM expression in nonhematopoietic cells contributes to VSV susceptibility and cytokine production

The increased survival of *SARM*$^{-/-}$ mice compared with WT mice after VSV infection appeared to be correlated with a blunted inflammatory response in the brain. Therefore, we generated BM chimeras to dissect out the contribution of hematopoietic and nonhematopoietic SARM-expressing cells to the inflammatory response in the brain. Strikingly, SARM deficiency in nonhematopoietic cells afforded protection from VSV (Fig. 4A), as *SARM*$^{-/-}$ recipients of either WT or *SARM*$^{-/-}$ BM were better able to survive VSV infection. In addition, cytokine and chemokine production was observed in WT→WT chimeras and *SARM*$^{-/-}$→WT chimeras, but not in *SARM*$^{-/-}$→ *SARM*$^{-/-}$ or WT→*SARM*$^{-/-}$ chimeras, indicating that WT nonhematopoietic cells were responsible for increased cytokine production in the brain (Fig. 4B). However, WT→WT chimeras showed higher levels for some cytokines compared with *SARM*$^{-/-}$→WT chimeras, indicating that SARM expression in BM cells may make some contribution to cytokine production. The observed mortality of WT mice is likely related to the inflammatory response generated by the cells of the nonhematopoietic compartment, because mice depleted of macrophages displayed viral replication and encephalitis similar to WT (24).

Neurons and microglia cooperate to induce cytokine production

Because susceptibility to VSV correlated with cytokine and chemokine production in the CNS, we examined the cell types responsible for chemokine production. We chose MCP-1 because it is known to be induced after injury and before neurodegeneration and infiltration (25, 26). Olfactory bulb sections confirmed the presence of MCP-1 staining in VSV-infected WT but not *SARM*$^{-/-}$ mice (Fig. 5A). Costaining with neuronal nuclei for neurons, CD11b for microglia, and GFAP for astrocytes indicated that both neurons and microglia from WT infected mice produced MCP-1 (Fig. 5B), with neurons being the predominant source.

Table I. Lack of upregulation of chemokines and IFN-inducible genes in VSV-infected *SARM*$^{-/-}$ mice

Score	Fold Change	Gene Symbol	Gene Name
		Upregulated in WT Compared with *SARM*$^{-/-}$	
26.9	3.1	Gbp2	Guanylate nucleotide binding protein 2
15.0	4.4	CXCL10	Chemokine (C-X-C motif) ligand 10
13.8	3.1	Gbp2	Guanylate nucleotide binding protein 2
10.2	3.2	Ifi205	IFN activated gene 205
10.2	8.1		CDNA clone IMAGE:5719021
9.5	3.2	Ifi203	IFN activated gene 203
9.2	6.0	Erdr1	Erythroid differentiation regulator 1
9.2	3.1	Gdpd1	Glycerophosphodiester phosphodiesterase domain containing 1
8.7	2.5	Ifi203	IFN activated gene 203, Ifi203
8.2	2.5	ISG15 like	ISG15 ubiquitin-like modifier
7.5	2.3	CCL5	Chemokine (C-C motif) ligand 5
7.4	7.2		RIKEN cDNA G530011O06 gene
7.1	3.4	Rsad2	Radical S-adenosyl methionine domain containing 2
7.1	6.8	Mid1	Midline 1
7.0	2.9	Rsad2	Radical S-adenosyl methionine domain containing 2
7.0	5.1	Slfn4	Schlafen 4
6.9	2.4	CD274	CD274 Ag
6.7	2.9	Mx1	Myxovirus resistance 1
6.7	2.6		DNA segment, Chr 14, ERATO Doi 668
6.7	2.4	Iigp1	IFN inducible GTPase 1
6.6	2.4	Ms4a4c	Membrane-spanning 4-domains, subfamily A, member 4C
6.0	3.0	Ms4a4b	Membrane-spanning 4-domains, subfamily A, member 4B
6.0	3.2		Predicted gene, EG633640
5.7	2.7	CXCL9	Chemokine (C-X-C motif) ligand 9
5.4	3.2	CCL12	Chemokine (C-C motif) ligand 12
5.4	3.8	Plac8	Placenta-specific 8
5.3	2.9	Rsad2	Radical S-adenosyl methionine domain containing 2
5.3	2.5	Ifi44	IFN-induced protein 44
5.1	2.8	Ms4a6d	Membrane-spanning 4-domains, subfamily A, member 6D
		Upregulated in SARM$^{-/-}$ Compared with WT	
52.4	42.0	Xaf1	XIAP associated factor 1
49.8	3.5	Wdfy1	WD repeat and FYVE domain containing 1
27.6	3.6	Wdfy1	WD repeat and FYVE domain containing 1
13.5	3.8		Transcribed locus, moderately similar to XP_001477892.1
11.8	3.8	Wdfy1	WD repeat and FYVE domain containing 1

WT and *SARM*$^{-/-}$ mice were infected intranasally with VSV, and brains were harvested at day 5 postinfection for microarray analysis. Genes showing >2-fold change between WT and *SARM*$^{-/-}$ mice are shown.

To determine what cell types are important for cytokine production, we cultured neurons, microglia, and astrocytes in vitro. Neurons and astrocytes produced only low levels of MCP-1 and TNF-α (Fig. 5C) in response to VSV infection. In contrast, microglia produced high levels of MCP-1 and TNF-α. Surprisingly, no difference in cytokine production was observed between WT and *SARM*$^{-/-}$ cells, suggesting that differences in cytokine production are not cell intrinsic. Consistent with our in vivo results, we did not observe any differences in viral replication in isolated neuron or macrophage cultures (data not shown). Because neuroinflammatory responses often require cooperation between neurons and glia, we infected mixed cell cultures with VSV to assess the production of cytokines. WT neurons cultured at a 10:1 ratio with WT microglia produced high levels of MCP-1 and TNF-α (Fig. 5D). In contrast, *SARM*$^{-/-}$ neurons cultured with *SARM*$^{-/-}$ microglia showed greatly diminished MCP-1 production (Fig. 5D, note 10-fold more microglia are present in Fig. 5C). To assess whether the interaction between neurons and microglia was unique, we cocultured neurons and astrocytes or neurons and macrophages. Neither astrocytes nor macrophages were able to reproduce the cytokine production observed when neurons and microglia were cocultured (Fig. 5D), suggesting that a unique interaction between neurons and microglia was required for cytokine production. However, at higher MOIs and later time points, we did observe low levels of TNF-α production and high levels of IFN-α production by macrophages that were not affected by the absence of SARM. The low level of cytokine production is likely due to potent suppression of host protein translation by the M protein because infection with the M51R mutant enhanced cytokine production (Supplemental Fig. 4). Microglia are thought to be maintained in the healthy CNS in an active resting state and express a wide variety of receptors that allow them to very rapidly respond to changes in homeostasis (27), which may explain their ability to produce cytokines during VSV infection.

Discussion

We have infected *SARM*$^{-/-}$ mice with a number of bacterial and viral pathogens to investigate a possible role of SARM in innate immunity. We have found that *SARM*$^{-/-}$ mice display normal responses to most pathogens tested but were dramatically protected from lethality and CNS damage from VSV infection. Normal responses to most infections support a role for SARM in specific CNS pathology consistent with its expression pattern. We also found that expression of SARM in nonhematopoietic cells was critical for lethality and cytokine production.

In contrast with our results, Szretter et al. (8) found that independently generated *SARM*$^{-/-}$ mice were more susceptible to West Nile virus infection. They similarly found reduced TNF-α production, but in contrast with our results observed more cell death in knockout animals. These results may reflect differences in the nature of the immune response required to clear specific

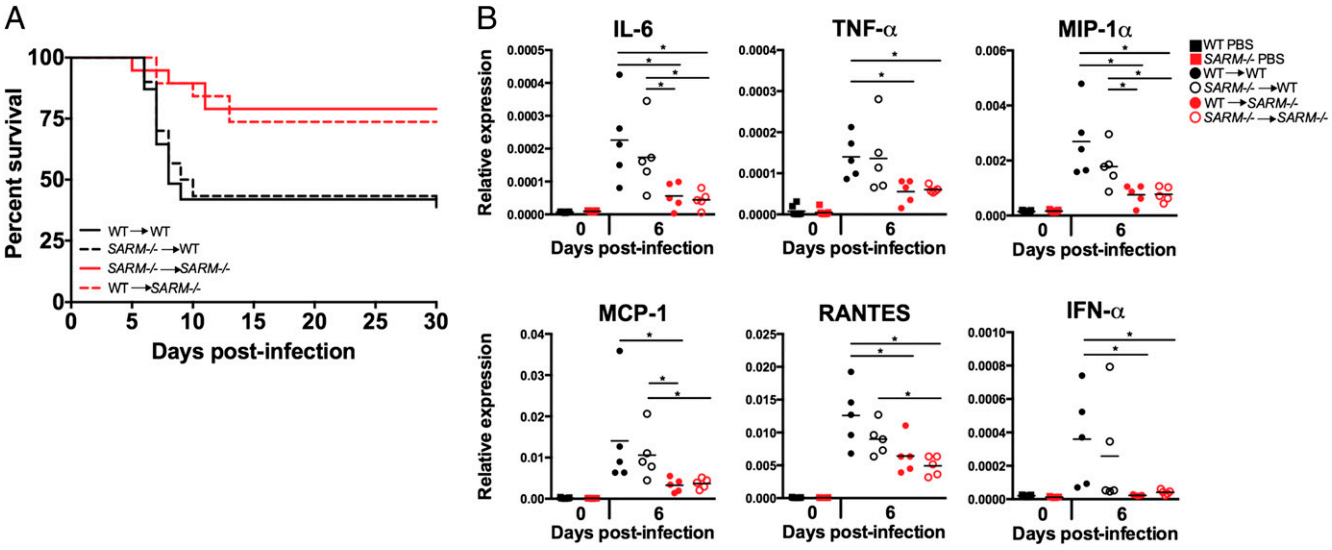

FIGURE 4. SARM expression is critical in nonhematopoietic cells. (**A**) WT recipients of bone marrow, irrespective of the genotype of bone marrow, were more susceptible to intranasal VSV infection. Thirteen of 30 $SARM^{-/-}$→WT mice survived VSV infection, as compared with 14/19 WT→$SARM^{-/-}$ mice, $p < 0.02$. Thirteen of 31 WT→WT and 15/19 $SARM^{-/-}$→$SARM^{-/-}$ mice survived VSV infection, $p < 0.02$. (**B**) qRT-PCR results of VSV-infected BM chimeras. WT recipients of BM express higher levels of cytokines at day 6 after VSV infection than $SARM^{-/-}$ ($n = 5$ per time point). Bars represent mean expression. WT and $SARM^{-/-}$ PBS controls from Fig. 3A are shown for comparison. *$p < 0.05$, Student t test.

pathogens (VSV versus West Nile virus) whereas limiting damage to the CNS. Differences in lethality may be a result of direct viral damage or immune-mediated damage (28). Cytokine production and infiltration of the CNS may be beneficial for clearance of WNV infection but may contribute to pathology during VSV infection. However, both studies support a positive role for SARM in cytokine production in the brain, with the outcome of infection differing depending on the viral infection. Mukherjee et al. (29) have also recently reported that $SARM^{-/-}$ mice are resistant to La Crosse virus infection and neuronal damage induced by the virus via a mechanism dependent on MAVS.

Osterloh et al. (9) have recently reported that both *Drosophila* and mouse SARM are required for injury-induced axonal cell death. Wallerian degeneration is an active cell death program akin to apoptosis with a well-established innate immune component that allows for clearance of debris from damaged neurons and subsequent nerve regeneration (12). Consistent with this, we observed less overall pathology and less neurodegeneration in $SARM^{-/-}$ VSV-infected animals. Importantly, we also observed a dramatic reduction in cytokine production, with neurons being the predominant source of cytokines. This supports a role for SARM in linking neuronal damage with the innate immune response. It is unclear whether neurodegeneration or cytokine production and infiltration are more relevant for in vivo protection, and this is difficult to assess experimentally because they are likely to be linked. Future work will address whether a specific cytokine or chemokine is responsible for pathogenesis, or a number of factors create a proinflammatory environment that leads to pathogenesis.

In addition to expression in neurons, low-level expression of SARM was observed in T cells from SARM-GFP BAC transgenic mice (7). Panneerselvam et al. (30) have recently reported that overexpression of SARM in 293T cells and $CD8^+$ T cells causes increased apoptosis via the intrinsic mitochondrial pathway. In addition, knockdown of SARM in CD8 T cells led to enhanced survival. Localization of SARM at the mitochondria and mitochondrial clustering have been reported when SARM is overexpressed (7). However, Osterloh (9) et al. report that endogenous Drosophila SARM-GFP is broadly localized to axons and not preferentially located at the mitochondria, and the poor quality of mouse Abs make localization hard to access. We did not observe any defects in T cell proliferation in vitro (Supplemental Fig. 3) or increased T cell accumulation in vivo (Fig. 5E), although differences may be apparent at later time points postinfection.

In vivo, we observed that neurons were the predominant source of cytokines, but we also observed cytokine production by microglia. In addition, it is important to note that microglia are predominantly of host origin in radiation bone marrow chimeras (31), so microglia may contribute to cytokine production. In isolated neuronal and microglial cultures, we were unable to observe differences in cytokine production in response to VSV infection, but our in vitro mixed neuronal cultures revealed a novel interaction between neurons and microglia leading to cytokine production. Activated microglia have been implicated in the pathogenesis of various CNS diseases, including Alzheimer's disease (32) and Parkinson's disease (33), as well as variety of different viral infections (34–36). Microglia have been described as the resident macrophage of the CNS because they share many similar characteristics and effector functions (37), but they are a distinct population arising from different precursors than macrophages. Recent lineage tracing has shown that mouse adult microglia are derived from primitive myeloid precursors that arise from the extraembryonic yolk sac and seed in the mouse brain (38) in a process that occurs before definitive hematopoiesis (39). Unlike adult mouse macrophages, microglia are self-renewing and are resistant to high doses of gamma-ray irradiation (40). Although astrocytes can also initiate and enhance inflammation in the CNS, our coculture experiments did not reveal a role for astrocytes in VSV-induced cytokine production.

The nature of the interaction between neurons and microglia leading to cytokine production requires further investigation. Microglia are thought to be the predominant source of cytokines in the brain, but recent evidence suggests that neurons are also capable of producing cytokines (41). Our in vivo cytokine staining suggests that both neurons and microglia produce cytokines during infection. Glial cells can contribute to neuroinflammatory responses through the generation of proinflammatory mediators, but they can also communicate with neurons bidirectionally via contact-mediated or se-

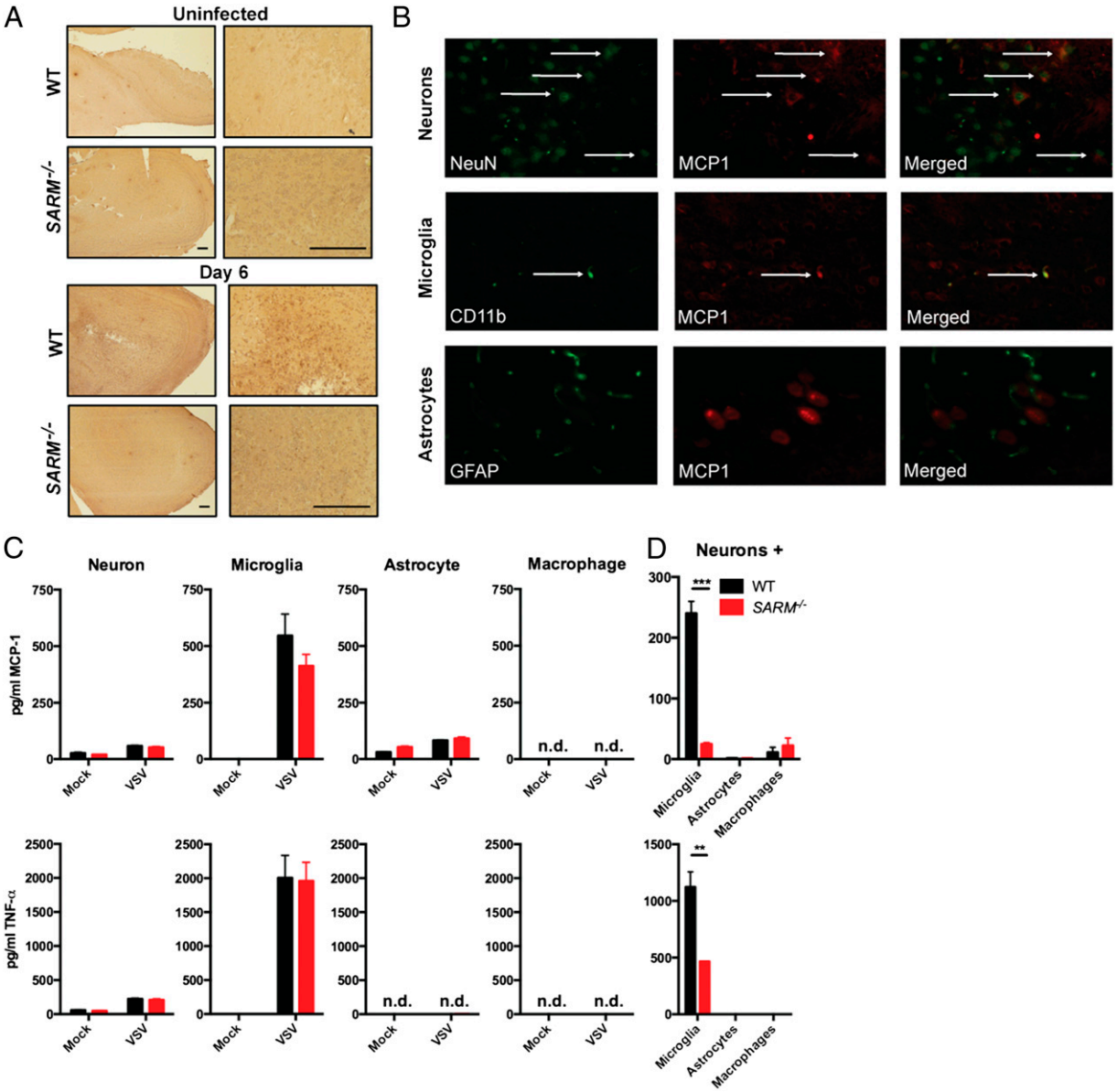

FIGURE 5. Neurons are the predominant source of chemokines. (**A**) Representative photomicrographs of olfactory bulb sections from mice infected intranasally with VSV at day 6 postinfection stained for MCP-1 are shown at ×4 (left) and ×63 (right) original magnification; scale bar, 200 μm. (**B**) Representative confocal microscopic images of MCP-1 (red) and neuronal nuclei (green, top), CD11b (green, middle), and GFAP (green, bottom) staining for neurons, microglia, and astrocytes, respectively, from mice infected intranasally with VSV at day 6 postinfection. (**C**) A total of 1.5×10^5 neurons, microglia, astrocytes, or macrophages were infected with VSV (MOI = 1) for 8 h and MCP-1 production measured by ELISA. (**D**) WT hippocampal neurons were cocultured with microglia, astrocytes, or macrophages at a 10:1 ratio (1.5×10^5 neurons to 1.5×10^4 glia), infected with VSV at an MOI of 1 for 8 h, and the supernatant was assayed for MCP-1 production. For (A) and (B), data are representative of five mice; for (C) and (D), bars represent SD $n = 4$, $^{**}p < 0.005$, $^{***}p < 0.0005$. n.d., Nondetectable.

creted factors to regulate the level of inflammatory responses. Many microglia-derived molecules can promote neurodegeneration, including IL-1β (42), reactive oxygen species (43), NO (44), glutamate (45), and ATP (46). In addition to soluble mediators, there could be a cell–cell contact requirement between neurons and microglia that is disrupted in SARM$^{-/-}$ neurons and microglia. The neuroimmunoregulatory CX3CL1–CX3CR1 interaction is a mechanism used by neurons to prevent aberrant microglia activation. Another neuroimmunoregulatory molecule is CD200, which is expressed on neurons. By interacting with its receptor, CD200R, on microglia, microglia are kept quiescent in the normal state and prevent phagocytosis (13). It is possible that loss of any of these cell–cell interactions can lead to microglia activation and an inflammatory response. Future experiments will address whether soluble factors or cell–cell contact are required for cytokine production and whether viral pathogen-associated molecular pattern or endogenous danger signals are upstream of SARM.

In summary, our data demonstrate that mammalian SARM plays a role in neurodegeneration during viral CNS infection. In addition, SARM plays a positive role in cytokine production similar to its *C. elegans* homolog. This is likely limited to infections of the CNS consistent with its expression pattern and its importance on nonhematopoietic cells. The data suggest that SARM is crucial for CNS injury and cytokine production in the CNS and may provide a link between neurodegeneration and the innate immune response. Therapeutic targeting of SARM may be beneficial in neurodegenerative diseases and CNS viral infection.

Acknowledgments

We thank Dr. Virginia Guillespie at the Comparative Pathology Diagnostic Laboratory at the Icahn Medical School at Mount Sinai for reading pathology slides. We also thank Richard Cadagan, Osman Lizardo, Huihong Li, and Xiuju Jiang for excellent technical assistance.

Disclosures

The authors have no financial conflicts of interest.

References

1. O'Neill, L. A., and A. G. Bowie. 2007. The family of five: TIR-domain-containing adaptors in Toll-like receptor signalling. *Nat. Rev. Immunol.* 7: 353–364.
2. Mink, M., B. Fogelgren, K. Olszewski, P. Maroy, and K. Csiszar. 2001. A novel human gene (SARM) at chromosome 17q11 encodes a protein with a SAM motif and structural similarity to Armadillo/beta-catenin that is conserved in mouse, Drosophila, and *Caenorhabditis elegans*. *Genomics* 74: 234–244.
3. Harris, T. W., I. Antoshechkin, T. Bieri, D. Blasiar, J. Chan, W. J. Chen, N. De La Cruz, P. Davis, M. Duesbury, R. Fang, et al. 2010. WormBase: a comprehensive resource for nematode research. *Nucleic Acids Res.* 38(Database issue): D463–D467.
4. Couillault, C., N. Pujol, J. Reboul, L. Sabatier, J. F. Guichou, Y. Kohara, and J. J. Ewbank. 2004. TLR-independent control of innate immunity in *Caenorhabditis elegans* by the TIR domain adaptor protein TIR-1, an ortholog of human SARM. *Nat. Immunol.* 5: 488–494.
5. Chuang, C. F., and C. I. Bargmann. 2005. A Toll-interleukin 1 repeat protein at the synapse specifies asymmetric odorant receptor expression via ASK1 MAPKKK signaling. *Genes Dev.* 19: 270–281.
6. Carty, M., R. Goodbody, M. Schröder, J. Stack, P. N. Moynagh, and A. G. Bowie. 2006. The human adaptor SARM negatively regulates adaptor protein TRIF-dependent Toll-like receptor signaling. *Nat. Immunol.* 7: 1074–1081.
7. Kim, Y., P. Zhou, L. Qian, J. Z. Chuang, J. Lee, C. Li, C. Iadecola, C. Nathan, and A. Ding. 2007. MyD88-5 links mitochondria, microtubules, and JNK3 in neurons and regulates neuronal survival. *J. Exp. Med.* 204: 2063–2074.
8. Szretter, K. J., M. A. Samuel, S. Gilfillan, A. Fuchs, M. Colonna, and M. S. Diamond. 2009. The immune adaptor molecule SARM modulates tumor necrosis factor alpha production and microglia activation in the brainstem and restricts West Nile Virus pathogenesis. *J. Virol.* 83: 9329–9338.
9. Osterloh, J. M., J. Yang, T. M. Rooney, A. N. Fox, R. Adalbert, E. H. Powell, A. E. Sheehan, M. A. Avery, R. Hackett, M. A. Logan, et al. 2012. dSarm/Sarm1 is required for activation of an injury-induced axon death pathway. *Science* 337: 481–484.
10. Friede, R. L. 1963. The relationship of body size, nerve cell size, axon length, and glial density in the cerebellum. *Proc. Natl. Acad. Sci. USA* 49: 187–193.
11. Wang, J. T., Z. A. Medress, and B. A. Barres. 2012. Axon degeneration: molecular mechanisms of a self-destruction pathway. *J. Cell Biol.* 196: 7–18.
12. Shamash, S., F. Reichert, and S. Rotshenker. 2002. The cytokine network of Wallerian degeneration: tumor necrosis factor-alpha, interleukin-1alpha, and interleukin-1beta. *J. Neurosci.* 22: 3052–3060.
13. Griffiths, M. R., P. Gasque, and J. W. Neal. 2010. The regulation of the CNS innate immune response is vital for the restoration of tissue homeostasis (repair) after acute brain injury: a brief review. *Int. J. Inflamm.* 2010: 151097.
14. Butchi, N. B., T. Woods, M. Du, T. W. Morgan, and K. E. Peterson. 2011. TLR7 and TLR9 trigger distinct neuroinflammatory responses in the CNS. *Am. J. Pathol.* 179: 783–794.
15. Wyss-Coray, T., and L. Mucke. 2002. Inflammation in neurodegenerative disease—a double-edged sword. *Neuron* 35: 419–432.
16. Björklund, A., and O. Lindvall. 2000. Self-repair in the brain. *Nature* 405: 892–893, 895.
17. Noda, M., Y. Doi, J. Liang, J. Kawanokuchi, Y. Sonobe, H. Takeuchi, T. Mizuno, and A. Suzumura. 2011. Fractalkine attenuates excito-neurotoxicity via microglial clearance of damaged neurons and antioxidant enzyme heme oxygenase-1 expression. *J. Biol. Chem.* 286: 2308–2319.
18. Matrosovich, M., T. Matrosovich, W. Garten, and H. D. Klenk. 2006. New low-viscosity overlay medium for viral plaque assays. *Virol. J.* 3: 63.
19. Kaech, S., and G. Banker. 2006. Culturing hippocampal neurons. *Nat. Protoc.* 1: 2406–2415.
20. Wang, T., T. Town, L. Alexopoulou, J. F. Anderson, E. Fikrig, and R. A. Flavell. 2004. Toll-like receptor 3 mediates West Nile virus entry into the brain causing lethal encephalitis. *Nat. Med.* 10: 1366–1373.
21. Huneycutt, B. S., I. V. Plakhov, Z. Shusterman, S. M. Bartido, A. Huang, C. S. Reiss, and C. Aoki. 1994. Distribution of vesicular stomatitis virus proteins in the brains of BALB/c mice following intranasal inoculation: an immunohistochemical analysis. *Brain Res.* 635: 81–95.
22. Ireland, D. D., and C. S. Reiss. 2006. Gene expression contributing to recruitment of circulating cells in response to vesicular stomatitis virus infection of the CNS. *Viral Immunol.* 19: 536–545.
23. Detje, C. N., T. Meyer, H. Schmidt, D. Kreuz, J. K. Rose, I. Bechmann, M. Prinz, and U. Kalinke. 2009. Local type I IFN receptor signaling protects against virus spread within the central nervous system. *J. Immunol.* 182: 2297–2304.
24. Steel, C. D., W. K. Kim, L. D. Sanford, L. L. Wellman, S. Burnett, N. Van Rooijen, and R. P. Ciavarra. 2010. Distinct macrophage subpopulations regulate viral encephalitis but not viral clearance in the CNS. *J. Neuroimmunol.* 226: 81–92.
25. Carroll, S. L., and P. W. Frohnert. 1998. Expression of JE (monocyte chemoattractant protein-1) is induced by sciatic axotomy in wild type rodents but not in C57BL/Wld(s) mice. *J. Neuropathol. Exp. Neurol.* 57: 915–930.
26. Perrin, F. E., S. Lacroix, M. Avilés-Trigueros, and S. David. 2005. Involvement of monocyte chemoattractant protein-1, macrophage inflammatory protein-1alpha and interleukin-1beta in Wallerian degeneration. *Brain* 128: 854–866.
27. Hanisch, U. K., and H. Kettenmann. 2007. Microglia: active sensor and versatile effector cells in the normal and pathologic brain. *Nat. Neurosci.* 10: 1387–1394.
28. Rivest, S. 2009. Regulation of innate immune responses in the brain. *Nat. Rev. Immunol.* 9: 429–439.
29. Mukherjee, P., T. A. Woods, R. A. Moore, and K. E. Peterson. 2013. Activation of the innate signaling molecule MAVS by bunyavirus infection upregulates the adaptor protein SARM1, leading to neuronal death. *Immunity* 38: 705–716.
30. Panneerselvam, P., L. P. Singh, V. Selvarajan, W. J. Chng, S. B. Ng, N. S. Tan, B. Ho, J. Chen, and J. L. Ding. 2013. T-cell death following immune activation is mediated by mitochondria-localized SARM. *Cell Death Differ.* 20: 478–489.
31. Ransohoff, R. M., and A. E. Cardona. 2010. The myeloid cells of the central nervous system parenchyma. *Nature* 468: 253–262.
32. Cameron, B., and G. E. Landreth. 2010. Inflammation, microglia, and Alzheimer's disease. *Neurobiol. Dis.* 37: 503–509.
33. Orr, C. F., D. B. Rowe, and G. M. Halliday. 2002. An inflammatory review of Parkinson's disease. *Prog. Neurobiol.* 68: 325–340.
34. Ovanesov, M. V., Y. Ayhan, C. Wolbert, K. Moldovan, C. Sauder, and M. V. Pletnikov. 2008. Astrocytes play a key role in activation of microglia by persistent Borna disease virus infection. *J. Neuroinflammation* 5: 50.
35. Chen, C. J., Y. C. Ou, S. Y. Lin, S. L. Raung, S. L. Liao, C. Y. Lai, S. Y. Chen, and J. H. Chen. 2010. Glial activation involvement in neuronal death by Japanese encephalitis virus infection. *J. Gen. Virol.* 91: 1028–1037.
36. Chauhan, V. S., S. R. Furr, D. G. Sterka, Jr., D. A. Nelson, M. Moerdyk-Schauwecker, I. Marriott, and V. Z. Grdzelishvili. 2010. Vesicular stomatitis virus infects resident cells of the central nervous system and induces replication-dependent inflammatory responses. *Virology* 400: 187–196.
37. Iadecola, C., and J. Anrather. 2011. The immunology of stroke: from mechanisms to translation. *Nat. Med.* 17: 796–808.
38. Ginhoux, F., M. Greter, M. Leboeuf, S. Nandi, P. See, S. Gokhan, M. F. Mehler, S. J. Conway, L. G. Ng, E. R. Stanley, et al. 2010. Fate mapping analysis reveals that adult microglia derive from primitive macrophages. *Science* 330: 841–845.
39. Orkin, S. H., and L. I. Zon. 2008. Hematopoiesis: an evolving paradigm for stem cell biology. *Cell* 132: 631–644.
40. Ajami, B., J. L. Bennett, C. Krieger, K. M. McNagny, and F. M. Rossi. 2011. Infiltrating monocytes trigger EAE progression, but do not contribute to the resident microglia pool. *Nat. Neurosci.* 14: 1142–1149.
41. Yang, G., Y. Meng, W. Li, Y. Yong, Z. Fan, H. Ding, Y. Wei, J. Luo, and Z. J. Ke. 2011. Neuronal MCP-1 mediates microglia recruitment and neurodegeneration induced by the mild impairment of oxidative metabolism. *Brain Pathol.* 21: 279–297.
42. Tolosa, L., V. Caraballo-Miralles, G. Olmos, and J. Lladó. 2011. TNF-α potentiates glutamate-induced spinal cord motoneuron death via NF-κB. *Mol. Cell. Neurosci.* 46: 176–186.
43. Chao, C. C., S. Hu, L. Ehrlich, and P. K. Peterson. 1995. Interleukin-1 and tumor necrosis factor-alpha synergistically mediate neurotoxicity: involvement of nitric oxide and of N-methyl-D-aspartate receptors. *Brain Behav. Immun.* 9: 355–365.
44. Bal-Price, A., and G. C. Brown. 2001. Inflammatory neurodegeneration mediated by nitric oxide from activated glia-inhibiting neuronal respiration, causing glutamate release and excitotoxicity. *J. Neurosci.* 21: 6480–6491.
45. Chen, C. J., Y. C. Ou, C. Y. Chang, H. C. Pan, S. L. Liao, S. Y. Chen, S. L. Raung, and C. Y. Lai. 2012. Glutamate released by Japanese encephalitis virus-infected microglia involves TNF-α signaling and contributes to neuronal death. *Glia* 60: 487–501.
46. Pascual, O., S. Ben Achour, P. Rostaing, A. Triller, and A. Bessis. 2012. Microglia activation triggers astrocyte-mediated modulation of excitatory neurotransmission. *Proc. Natl. Acad. Sci. USA*.109: E197–E205.